Available online at www.sciencedirect.com
SCIENCE DIRECT
Journal of Photochemistry and Photobiology A: Chemistry 181 (2006) 348–356
Journal of Photochemistry and Photobiology A:Chemistry
www.elsevier.com/locate/jphotochem

Different mechanisms both lead to the production of the naphthalene–OH adduct in the 355 nm and 266 nm laser flash photolysis of the mixed aqueous solution of naphthalene and nitrous acid

Bin Ouyang, Haojie Fang, Wenbo Dong *, Huiqi Hou *

Department of Environmental Science and Engineering, Institute of Environmental Science, Fudan University, Handan Road 220, Shanghai 200433, PR China

Received 18 July 2005; received in revised form 3 October 2005; accepted 15 December 2005
Available online 24 January 2006

Abstract

The 355 nm and 266 nm nanosecond laser flash photolysis of the mixed aqueous solution of naphthalene (Np) and nitrous acid (HNO_2) were performed to investigate the photo-initiated microscopic reactions in this binary component system. Following the 355 nm laser flash, HNO_2 was readily photolyzed to NO and OH, and the latter fragment added to the Np ring to form the Np–OH adduct at the rate constant of $(1.1 \pm 0.1) \times 10^{10}\ M^{-1}\ s^{-1}$. Following the 266 nm laser flash, Np was populated first to its lowest excited singlet state (S_1) and then to its lowest excited triplet state (T_1) via intersystem crossing. Np(S_1) and Np(T_1) both formed the $[Np\cdots HNO_2]^*$ exciplex with HNO_2, and the fast dissociation of this exciplex again produced the Np–OH adduct. The second-order quenching rate constants of Np(S_1) and Np(T_1) by HNO_2 were measured to be $(6.0 \pm 0.2) \times 10^9\ M^{-1}\ s^{-1}$ and $(4.8 \pm 0.2) \times 10^9\ M^{-1}\ s^{-1}$, respectively. It was very interesting to conclude that although both the 355 nm and the 266 nm irradiation of the mixed aqueous solution of Np and HNO_2 produced the Np–OH adduct, the mechanisms leading to this species varied essentially for the two cases. This work suggested an unexpected way of releasing OH by HNO_2 other than its direct photolysis, namely via forming exciplex with the excited Np (and possibly other polycyclic aromatic hydrocarbons, PAHs) in the environment.

Keywords: Nitrous acid; Naphthalene; Naphthalene–OH adduct; Laser flash photolysis; Exciplex

1. Introduction

The absorption of nitrous acid (HNO_2) towards the 290–400 nm sunlight followed by an immediate release of OH was first reported by Cox [1]. Photolysis of HNO_2 was identified as one of the most important sources of OH with a quantum yield of near unity in the atmosphere [2,3]. There were also some reports on the aqueous photochemistry of HNO_2 [4–6], suggesting a similar photolysis process but a much lower quantum yield of OH than that in the gas phase. Admittedly, the photochemistry of HNO_2 in the environment was studied in a relatively thorough and complete manner that left few new fields to be cultivated.

The reactions of OH with the atmospheric organic pollutants in either the gas phase or the aqueous droplets constitute one of the major removal pathways of these substances [2,3]. The gas-phase electrophilic adduct of OH to the aromatic rings has been subjected to long and persistent researches and was recently reviewed by Atkinson and Arey [7]. The liquid-phase OH reactions with the aromatic substrates benefited a lot from the development of the pulse radiolysis technique [8]. The product, namely the OH adducts generally possess strong absorptions above 300 nm, which facilitates the probing of these intermediates using the UV–vis analyzing light source. The OH-initiated oxidations result in the hydroxylation and ring cleavage of the aromatic compounds.

We have previously studied the 355 nm laser flash photolysis of the aqueous solution of HNO_2. The transient absorption of the photolysis fragment OH radical was snapped immediately after the laser pulse [9]. This provides an alternative generation

* Corresponding authors. Tel.: +86 21 6564 2293/2030; fax: +86 21 6564 3849.
E-mail addresses: oybboy@yahoo.com.cn, fdesi@fudan.edu.cn (H. Hou).

1010-6030/$ – see front matter © 2005 Elsevier B.V. All rights reserved.
doi:10.1016/j.jphotochem.2005.12.017

method of OH radicals for laboratory researches besides the pulse radiolysis or the photolysis of H_2O_2.

When naphthalene was coexistent with HNO_2 in the solution, OH added to the naphthalene (Np) ring readily and led to the formation of the Np–OH adduct [8]. Np was transparent towards the 355 nm laser, so the radical reactions in this case were solely triggered by the photolysis of HNO_2. Questions and interests thus arose, i.e. what would happen if the photochemical reactions were provoked by the excitation of Np instead of HNO_2.

In this paper, we selectively excited HNO_2 and Np using the 355 nm and the 266 nm light, i.e. the third and the fourth harmonic of the Nd:YAG laser and through this means separately investigated the Np-initiated and the HNO_2-initiated photochemical reactions in the mixed aqueous solution of Np and HNO_2. What really intrigued us was that although the reaction mechanisms differed dramatically, the Np–OH adduct was formed in both cases. The reaction mechanisms leading to the formation of the Np–OH adduct in both the 266 nm and the 355 nm irradiation cases were postulated, as presented in the main text.

2. Experimental

The components of the laser flash photolysis instrument have been introduced elsewhere [9]. Besides, the 266 nm output has an FWHM of 5 ns and a maximum output of 70 mJ pulse^{-1}. The typical laser pulse energy applied in the 266 nm irradiation case was 4.8 ± 0.2 mJ.

Naphthalene, $NaNO_2$ and $HClO_4$ were of analytical grade. The water was triply distilled. pH of the sample solutions was adjusted to be 1.5 by adding $HClO_4$ to make more than 98.5% NO_2^- exist in the form of HNO_2 [9]. Unless specially addressed, all of the sample solutions were deoxygenated through 30 min vigorous bubbling of >99.999% N_2.

The experiments were carried out under flow conditions with a sample temperature of $20 \pm 2\,^{\circ}C$.

3. Results and discussion

3.1. Ground-state UV absorptions of Np and HNO_2 in the aqueous phase

The ground-state UV absorption spectra of Np (1.5×10^{-4} M) and HNO_2 (7×10^{-3} M) in the aqueous phase were shown in Fig. 1. Np exhibited strong $\pi^* \leftarrow \pi$ absorptions in the 260–320 nm region, while HNO_2 exhibit $\pi^* \leftarrow n$ absorptions in the 300–400 nm. The molar extinction coefficients (ε) of Np at 266 nm and of HNO_2 at 355 nm were 5140 $M^{-1}\,cm^{-1}$ and 41.7 $M^{-1}\,cm^{-1}$, respectively. It was also clear from Fig. 1 that the absorptions of Np at 355 nm and of HNO_2 at 266 nm were both negligible. This assures the "selective" excitation of one specific solute at 355 nm and 266 nm, respectively.

We should note that the UV absorption of Np was not affected by the acidity of the solution. Moreover, Np ($1–2 \times 10^{-4}$ M) and HNO_2 ($2–300 \times 10^{-4}$ M) did not form any ground-state complexes based on the fact that the UV–vis absorption spectrum of the mixed aqueous solution of Np and HNO_2 was exactly the sum of those of the individual Np and HNO_2 solutions.

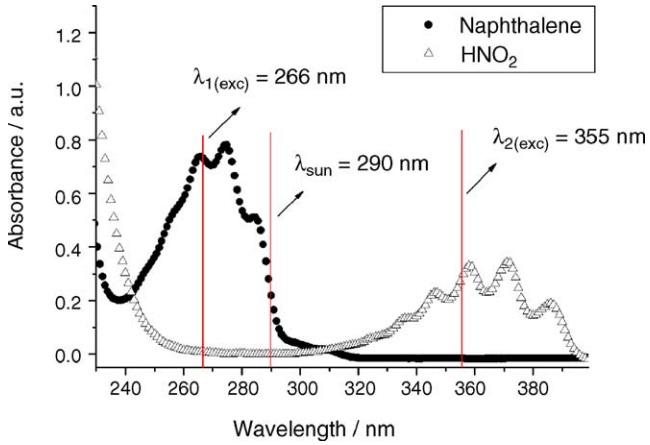

Fig. 1. The ground-state UV absorption spectra of 1.5×10^{-4} M Np and 7×10^{-3} M HNO_2 in the aqueous phase at pH 1.5.

3.2. Three hundred and fifty-five nanometer laser flash photolysis of the mixed aqueous solution of Np and HNO_2

HNO_2 was the only absorber in the 355 nm excitation mode and dissociated readily to form OH and NO at a quantum yield of 0.25 ± 0.03 [9]. When Np was added into the solution, the formation of the Np–OH adduct was observed in the 290–400 nm probing region [10]. The addition of excessive efficient OH scavengers, e.g. ethanol or *iso*-propanol strongly suppressed the formation of this adduct. Therefore the "free" OH radical from the photolysis of HNO_2 was exactly the precursor of the Np–OH adduct. It should be mentioned that HNO_2 competitively scavenged OH radical against Np as well. The reaction sequence was summarized in Scheme 1 (355 nm irradiation).

Based on Scheme 1, the pseudo-first-order growth rate constant, i.e. k_{obs}, of the Np–OH adduct at its absorption peak ($\lambda_{max} = 320$ nm) should equal to $k_2 \times [Np] + k_3 \times [HNO_2]$. By fixing [Np] at 1.2×10^{-4} M and varying [HNO_2], we got a linear plot of k_{obs} against [HNO_2], as shown in Fig. 2. The intercept and slope of the line correspond to $k_2 \times [Np]$ and k_3, respectively. k_2 and k_3 were then derived to be $(1.1 \pm 0.1) \times 10^{10}\,M^{-1}\,s^{-1}$ and $(8.5 \pm 1.0) \times 10^{8}\,M^{-1}\,s^{-1}$, respectively.

The value of k_{OH+Np} from this work agreed quite well with the results of Zevos and Sehested [11] and Roder et al. [12], viz. $1.2 \times 10^{10}\,M^{-1}\,s^{-1}$. This implied diffusion-controlled electrophilic attack of OH to the Np ring and was quite reasonable when considering a parallel one by OH to the benzene ring [13].

The reports on k_{OH+HNO_2} in the aqueous phase were scarce, however. To the best of our knowledge, only one value, viz. $1.0 \times 10^{9}\,M^{-1}\,s^{-1}$ was reported by Rettich through a steady-

$$HNO_2 + h\nu \rightarrow OH + NO \qquad \Phi = 0.25\ [9] \qquad (R.1)$$

$$OH + Np \xrightarrow{k_2} \text{Np-OH adduct} \qquad (R.2)$$

$$OH + HNO_2 \xrightarrow{k_3} NO_2 + H_2O \qquad (R.3)$$

Scheme 1.

state irradiation study in 1978 [14]. Clearly, our value agreed quite well with that of Rettich despite the different experiment methods applied. The other value commonly employed in the liquid-phase studies [4,6] was $2.8 \times 10^9\ M^{-1}\ s^{-1}$, which was not measured independently but was borrowed from the gas-phase report by Jenkin and Cox [15]. Therefore, the latter value was subject to more uncertainties since the presence of solvent molecules may affect the rate of the acid hydrogen abstractions by OH radical remarkably.

For a further check of k_{OH+HNO_2}, we turned to the other system where competition kinetics of OH between Cl^- and HNO_2 was built. Cl^- was well known to capture OH in acidic solutions [16]. In this case, $[Cl^-]$ was fixed to be 1.0×10^{-2} M and pH to be 1.5. By plotting the pseudo-first-order growth rate constant of $Cl_2^{\bullet -}$ at 340 nm against $[HNO_2]$, we derived another value, i.e. $(9.6 \pm 0.9) \times 10^8\ M^{-1}\ s^{-1}$, for k_2 (see Fig. 2). This approximates the one we got in the Np + HNO_2 system. An averaged rate constants, $(9.0 \pm 0.5) \times 10^8\ M^{-1}\ s^{-1}$ was recommended here for the rate constant of the $OH + HNO_2 \rightarrow H_2O + NO_2$ reaction in the aqueous phase.

By comparison of the rate constants of the hydrogen abstraction from HNO_2 by OH, $SO_4^{\bullet -}$ ($1.6 \times 10^8\ M^{-1}\ s^{-1}$ [17]) and NO_3 ($8.0 \times 10^6\ M^{-1}\ s^{-1}$ [18]), we observed declining abstraction capacity as $OH > SO_4^{\bullet -} > NO_3$. This trend was similar to that of the hydrogen abstraction from alcohols by these oxidative radicals and again implied that OH radical was among them the most powerful hydrogen abstraction agent.

3.3. Two hundred and sixty-six nanometer laser flash photolysis of the mixed aqueous solution of Np and HNO_2

3.3.1. Production of unidentified intermediate in the 266 nm laser flash photolysis of the mixed aqueous solution of Np and HNO_2

Following the 355 nm laser flash photolysis studies, we moved our focuses further to the 266 nm irradiation case. The

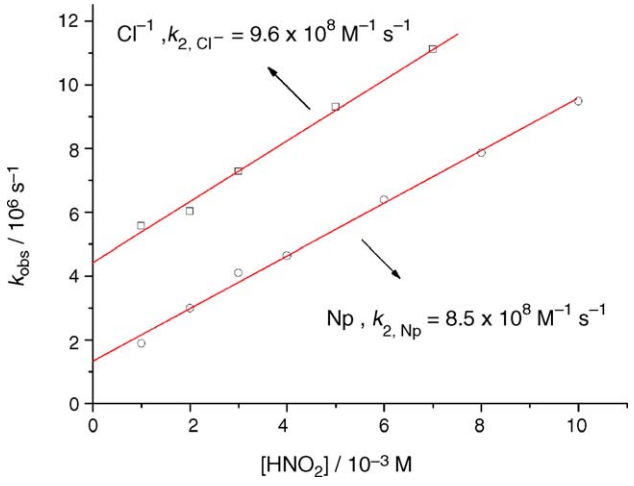

Fig. 2. Determination of the rate constant of the reaction $OH + HNO_2 \rightarrow NO_2 + H_2O$ in the aqueous phase using either Np or Cl^- as the competitive OH scavenger against HNO_2. $k_{2,Np}$ and k_{2,Cl^-} represent the slope of the two lines. For details, see Section 3.2.

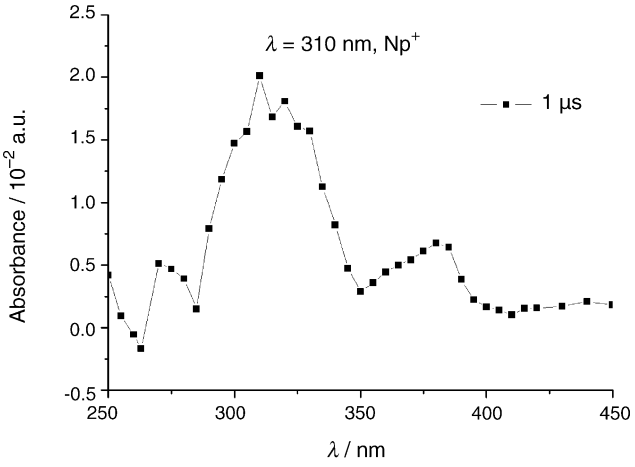

Fig. 3. Transient absorption spectra recorded at $t = 1$ μs after the laser flash photolysis of aqueous solution containing 1.5×10^{-4} M Np and 1×10^{-3} M HNO_2. The "obtruding" tip at λ = 310 nm reflected the remaining Np^+ in the solution, see Section 3.3.3 for detailed analysis.

dominant absorber changed from HNO_2 in the 355 nm case to Np in the 266 nm one.

Fig. 3 showed the transient absorption spectra recorded at $t = 1$ μs after the 266 nm laser flash photolysis of the mixed aqueous solution of 1.5×10^{-4} M Np and 1×10^{-3} M HNO_2. It attracted our intense interests in respect that despite some minor differences, the spectra resembled that of the Np–OH adduct to a striking extent [11,12].

In the meanwhile, two uncertainties remained unresolved as following:

(1) Was the intermediate in Fig. 3 the real Np–OH adduct?
(2) What was the precursor of the intermediate in Fig. 3? Both the excited Np and the Np radical cation (Np^+) were generated in the laser pulses (Section 3.3.2), but which one of them was responsible for the new intermediate?

To elucidate these problems, we made detailed spectral and kinetic analysis in Sections 3.3.2–3.3.4.

3.3.2. Elementary photochemical processes that populate the lowest excited singlet and triplet Np, together with the photoionization that leads to Np^+

It was widely acknowledged that excitation of the $\pi^* \leftarrow \pi$ absorption band of the polycyclic aromatic hydrocarbons (PAHs) first leads to the population of the higher excited singlet states (S_n). Then a fast internal conversion (IC) process occurs on the time scale of picosecond and degenerates the S_n state to S_1. S_1 thereafter converts to T_1 via intersystem crossing (ISC) that usually occurs on the time scale of ns ~ μs [19].

For Np, the $S_n \rightarrow S_1$ transition was so fast that we could not probe Np(S_n) directly using the ns spectrometer. Therefore, the intermediate we snapped immediately after the laser pulse can only be Np(S_1). Strong fluorescence with $\tau = (43 \pm 4)$ ns was observed in the 300–400 nm region. This corresponded to the $S_1 \rightarrow S_0$ transition [20]. Accompanying this transition was the

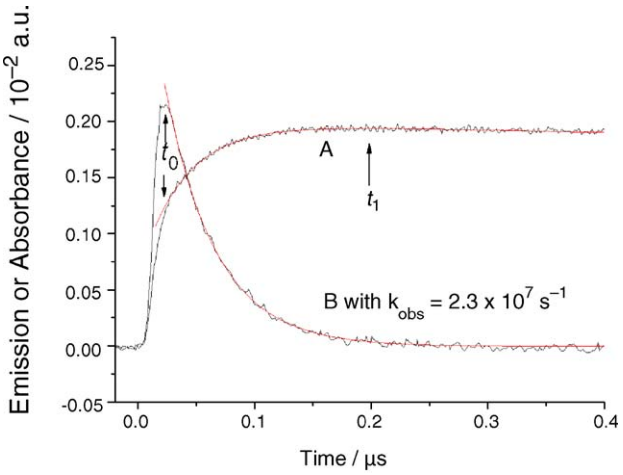

Fig. 4. Growth curve (A) of the transient absorption of Np(T_1) at 412 nm and decay curve (B) of the fluorescence of Np(S_1) at 320 nm recorded following the 266 nm laser flash photolysis of 1.5×10^{-4} M aqueous solution of Np. Clearly they proceeded at synchronous paces. t_0 denotes the end of the laser pulse when the Np(S_1) absorption was recorded and t_1 was the time point when the Np(T_1) absorption was recorded. The excitation laser pulse energy was 4.8 ± 0.2 mJ.

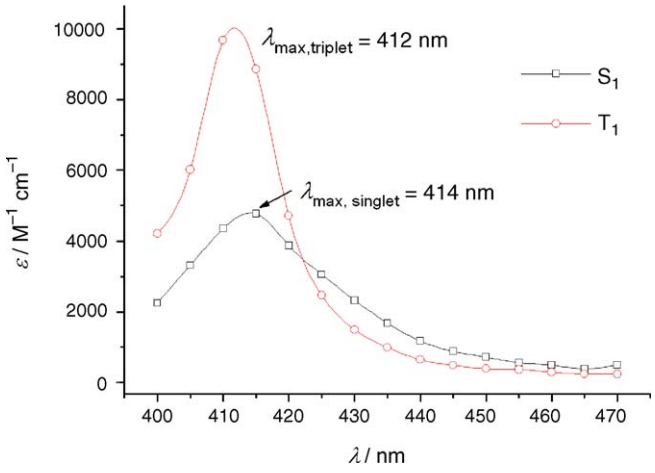

Fig. 5. The transient absorption spectra of Np(S_1) and Np(T_1) in aqueous solution.

$S_1 \rightarrow T_1$ process. Due to a larger molar extinction coefficient of Np(T_1) as compared with that of Np(S_1) at 410 nm, the transient absorption curve was appearing as a growth one, as shown in Fig. 4. The growth rate agreed quite well with that of the fluorescence decay, which again supported its assignment to Np(T_1). The whole process was summarized in reaction ((R.4)–(R.6)).

$$\mathrm{Np(S_0)} + h\nu \rightarrow \mathrm{Np(S_n)} \xrightarrow{\text{fast IC}(\approx \text{ps})} \mathrm{Np(S_1)} \quad \text{(R.4)}$$

$$\mathrm{Np(S_1)} \xrightarrow{\text{IC}} \mathrm{Np(S_0)} + h\nu_f \quad \text{(R.5)}$$

$$\mathrm{Np(S_1)} \xrightarrow{\text{ISC}} \mathrm{Np(T_1)} \quad \text{(R.6)}$$

According to Grabner et al., the molar extinction coefficient of Np(T_1) at 412 nm was $\varepsilon_{\mathrm{Np(T_1)},412\,\mathrm{nm}} = 10,050\,\mathrm{M^{-1}\,cm^{-1}}$ and the ISC quantum yield was $\Phi_{S_1 \rightarrow T_1} = 0.789$ [20]. On this basis, the molar extinction coefficient of Np(S_1), $\varepsilon_{\mathrm{Np(S_1)},\lambda}$, at λ can be derived using expression (7).

$$\varepsilon_{\mathrm{Np(S_1)},\lambda} = \frac{A_{\mathrm{Np(S_1)},\lambda} \cdot \Phi_{S_1 \rightarrow T_1} \cdot \varepsilon_{\mathrm{Np(T_1)},412\,\mathrm{nm}}}{A_{\mathrm{Np(T_1)},412\,\mathrm{nm}}} \quad (7)$$

$A_{\mathrm{Np(S_1)},\lambda}$ was the transient absorbance of Np(S_1) recorded at t_0, i.e. the time point at which the laser pulse ended and $A_{\mathrm{Np(T_1)},412\,\mathrm{nm}}$ was the transient absorbance of Np(T_1) recorded at t_1, the time point at which the Np(S_1) → Np(T_1) intersystem crossing finished (Fig. 4). The absorption spectra of Np(S_1) and Np(T_1) were shown in Fig. 5. The one of Np(T_1) in the aqueous phase has been reported previously [20], but the one of Np(S_1) in this phase is not available in the literature. Similar to that of the ground-state Np, the absorption spectra of Np(S_1) and Np(T_1) were not affected by the acidity of the solution either.

There were actually some reports on the absorption spectra of Np(S_1) and Np(T_1) in different solvents, most of which being organic ones [20–22]. Interestingly, although the solvent properties may vary dramatically and as a consequence $\varepsilon_{\mathrm{max,Np(T_1)}}$ and $\varepsilon_{\mathrm{max,Np(S_1)}}$ changes fiercely, the quotient of two values was always constant, i.e. near 2. This phenomenon needs to be subjected to further theoretical analysis.

Besides the population of the excited Np, photoionization occurs inevitably. Earlier investigation by Steeken et al. proposed the ionization to be a bi-photon process [23], but the more recent examination by Vialaton et al. revealed that it could also proceed via the single-photon process with a corresponding quantum yield of 0.02 [24]. The two channels were incorporated in reaction (R.8).

$$\mathrm{Np} + (n)h\nu \rightarrow \mathrm{Np^+}, \quad n = 1, 2 \quad \text{(R.8)}$$

Since the absorptions of Np^+ and Np(T_1) overlap, Steenken et al. used O_2 to quench the latter species and thus got the "pure" absorption spectra of Np^+ [23]. We followed this method in order to record the Np^+ signal. Owing to a much smaller quantum yield of Np^+ than that of Np(T_1), the peak transient absorbance of Np^+ was remarkably lower than that of Np(T_1), i.e. 5×10^{-3} versus 1.9×10^{-1}. We should note that the excitation laser energy per pulse was kept constant at 4.8 mJ when recording Np(T_1) and Np^+. The absorption spectrum of Np^+ we recorded in the aqueous phase agreed quite well with that of Steenken et al. [23] and was thus not included in this paper.

3.3.3. *Quenching of Np(T_1) by HNO_2 with Np–OH adduct formed*

When HNO_2 was added into the aqueous solution of Np, the decay of the transient absorption of Np(T_1) at 412 nm was remarkably accelerated. Linear correlation was confirmed when plotting the pseudo-first-order decay rates of the Np(T_1) absorption against [HNO_2], as illustrated in Fig. 6. By reading the slope of the line, we derived the quenching rate constant of Np(T_1) by HNO_2 to be $k_{\mathrm{Np(T_1)+HNO_2}} = (4.8 \pm 0.2) \times 10^9\,\mathrm{M^{-1}\,s^{-1}}$.

In contrast with the O_2 quenching of Np(T_1) where a nearly 100% physical quenching was met [25,26], the HNO_2 quenching clearly exhibited a chemical quenching property, since new intermediate emerged in the λ < 400 nm region immediately after the Np(T_1) disappeared, as already stated in Section 3.3.1.

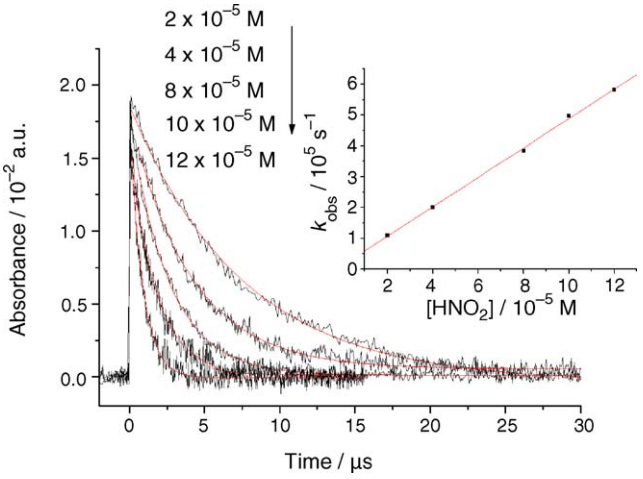

Fig. 6. Acceleration of the decay of the 412 nm Np(T_1) absorption by adding HNO_2. Inset: linear dependence of the pseudo-first-order decay rate of the Np(T_1) absorption on [HNO_2].

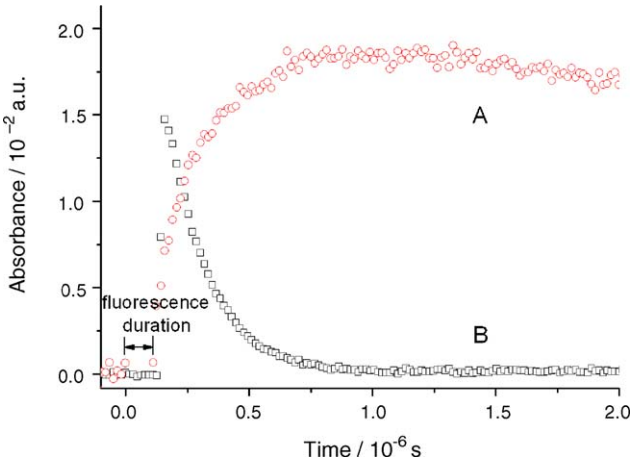

Fig. 8. Growth curve of the new intermediate at 320 nm (A) and the "scaled (/10)" decay curve of Np(T_1) at 412 nm (B), following the laser flash photolysis of 1.5×10^{-4} M Np and 1×10^{-3} M HNO_2 aqueous solution.

Although Np^+ was inevitably involved (but surely in a minor role) in the 266 nm photochemical processes, the new intermediate was by no means the reaction product of Np^+ with H_2O, Np or HNO_2. The reasons were listed as follows:

(1) Np^+ decayed very slowly in aqueous solution at pH 1.5. Fig. 7 was the decay curve of Np^+ at $\lambda_{max} = 310$ nm. According to Steenken et al., Np^+ disappears in water via reaction with H_2O and Np [23]. Therefore, it was reasonable to fit the Np^+ decay in Fig. 7 with a single exponential decay function since [Np] and [H_2O] $\gg$ [Np^+]. This yielded the first-order rate constant $k_{obs} = 2.9 \times 10^4$ s^{-1}. On this ground, the reaction of Np^+ with H_2O and Np was too slow to account for the new intermediate, whose growth was generally finished within 10 μs.

(2) Np^+ reacts with OH^- at $k = 2.4 \times 10^8$ M^{-1} s^{-1} [23]. But note that the pH was fixed at 1.5. As a result the [OH^-] was too low (<10^{-12} M) to react with Np^+ significantly.

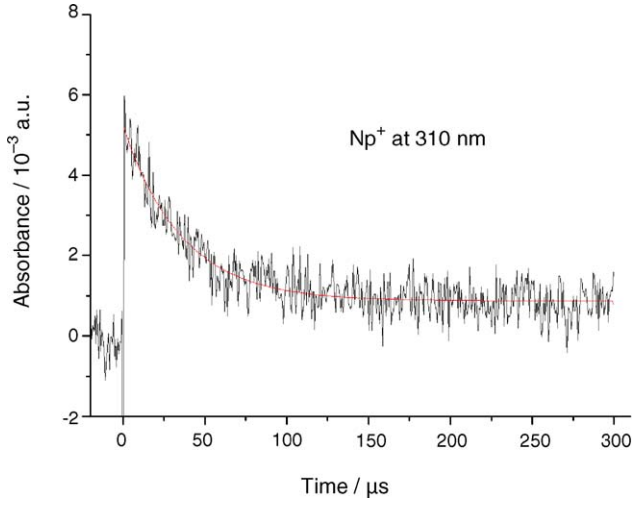

Fig. 7. The decay curve of Np^+ at 310 nm following the 266 nm laser flash photolysis of O_2-saturated 1.5×10^{-4} M aqueous solution of Np. It should be noted that Np(T_1) has disappeared in very early stages (0–1 μs).

(3) $SO_4^{\bullet -}$ oxidized Np readily to Np^+ via direct electron transfer [23]. After the 266 nm laser flash photolysis of air-saturated solution containing 0.1 M $K_2S_2O_8$ and 5×10^{-5} M Np (at pH 1.5), the formation of Np^+ was very easily observed. By gradually adding HNO_2 into the solution, the decay rate of Np^+ was indeed accelerated, with a second-order rate constant of $(1.4 \pm 0.3) \times 10^8$ M^{-1} s^{-1}. If the new intermediate indeed stemmed from the reaction $Np^+ + HNO_2$, its growth rate should correspond well with the decay of Np^+. This was not true, however, because the second-order growth rate constant of the intermediate against [HNO_2] was found to be on the order of 10^9 M^{-1} s^{-1}, which obviously exceeded the $Np^+ + HNO_2$ rate constant.

Fig. 8 shows the "scaled (/10)" decay of the Np(T_1) absorption at 412 nm and the growth of the new intermediate at 320 nm following the laser flash photolysis of the aqueous solution containing 1.5×10^{-4} M Np and 1×10^{-3} M HNO_2. Clearly they were proceeding synchronously. We carefully chose 320 nm to monitor the new intermediate because the absorption of Np^+ at this wavelength could be neglected [23]. It was worthy of noting that as [HNO_2] varied, both the growth and the decay rates changed correspondingly but were always kept in the same paces. This indicated that the new intermediate did come from the reaction Np(T_1) + HNO_2.

Fig. 3 was the transient absorption spectra we recorded at $t = 1$ μs after the laser flash photolysis of the aqueous solution containing 1.5×10^{-4} M Np and 1×10^{-3} M HNO_2. At this time point, Np(T_1) disappeared completely (see Fig. 6), but owing to a much slower reaction rate between Np^+ and HNO_2, 90% Np^+ stayed in the solution at $t = 1$ μs. This was further evidenced by the small "obtruding" tip at $\lambda = 310$ nm, i.e. the absorption peak of Np^+, in Fig. 3.

By subtracting the "known" absorption of Np^+ from Fig. 3, new transient absorption spectra was acquired, which was shown in Fig. 9. Co-plotted were the absorption spectra of the Np–OH adduct reported by different authors, virtually using different

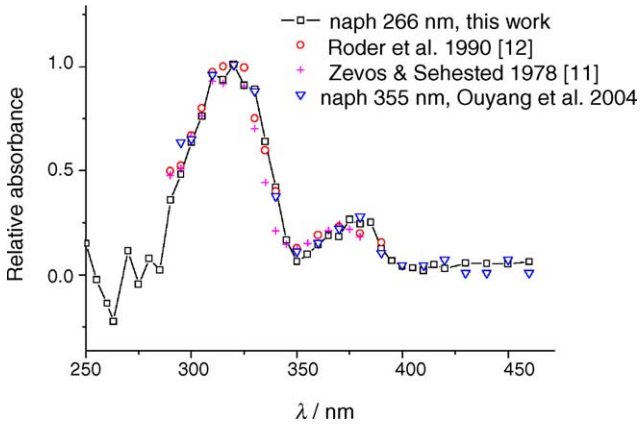

Fig. 9. Transient absorption spectra derived from Fig. 3 after the subtraction of the Np^+ absorption. Co-plotted was the absorption spectra of the Np–OH adduct reported by different authors using different OH sources (pulse radiolysis or photolysis of HNO_2).

methods. Note that for comparison purpose, the absorbance was adjusted to a same peak height at 320 nm. The strong resemblance between the spectra in Fig. 9 suggested that the new intermediate from the reaction of $Np(T_1) + HNO_2$ may be assigned to the Np–OH adduct.

To make this assignment more convincing, we examined the reactivity of this intermediate towards O_2 and HNO_2:

(1) The decay of the new species (monitored at 320 nm) was enhanced by the presence of O_2, as shown in Fig. 10. The second-order reaction rate constant of this species with O_2 was determined to be $(5.2 \pm 0.6) \times 10^8\ M^{-1}\ s^{-1}$, in excellent agreement with the one of the Np–OH + O_2 reaction, $(5.0 \pm 0.5) \times 10^8\ M^{-1}\ s^{-1}$, as reported by Roder et al. [12].

(2) The decay of the new species was also enhanced by increasing $[HNO_2]$. This was similar to the 355 nm irradiation case, where the increase of $[HNO_2]$ could accelerate the decay of the Np–OH adduct. Moreover, HNO_2 reacted with the intermediate (in the 266 nm case) at the rate constant of $(7.5 \pm 1.5) \times 10^7\ M^{-1}\ s^{-1}$, very close to the $(9.0 \pm 2.0) \times 10^7\ M^{-1}\ s^{-1}$ for the HNO_2 + Np–OH reaction derived in the 355 nm case.

To summarize, both the transient absorption spectra and the reactivity of the new species towards O_2 and HNO_2 agreed well with those of the Np–OH adduct. This convinced us that *this species was exactly the Np–OH adduct*.

3.3.4. Quenching of $Np(S_1)$ by HNO_2 with Np–OH again formed

In the absence of quenchers, $Np(S_1)$ decayed at $k_0 = 2.3 \times 10^7\ s^{-1}$ and emitted strong fluorescence in the 300–400 nm region [19]. The decay of the fluorescence was quickened by adding $[HNO_2]$. The linear relationship between the decay rate of the fluorescence and $[HNO_2]$ suggested that HNO_2 was capable of quenching $Np(S_1)$ as well, as suggested in Fig. 11. The rate constant for the reaction of $Np(S_1) + HNO_2$ was derived to be $(6.0 \pm 0.2) \times 10^9\ M^{-1}\ s^{-1}$ by reading the slope of k_{obs} against $[HNO_2]$.

When $[HNO_2]$ was low, e.g. $\leq 1 \times 10^{-3}$ M, $Np(S_1)$ disappeared mainly via ISC process to $Np(T_1)$. As long as $[HNO_2]$ was higher than 1×10^{-2} M, however, the HNO_2 quenching process overwhelmed the ISC process and would thus strongly cut the production of $Np(T_1)$. By this virtue, it was possible for us to examine the $Np(S_1) + HNO_2$ reaction separately.

To this end, the aqueous solution of 1.5×10^{-4} M Np + 2×10^{-2} M HNO_2 was photolyzed. Fig. 12 shows the transient absorption curve recorded at $\lambda = 290$ nm. We did not choose 320 nm because of the interference of the strong fluorescence of $Np(S_1)$ at this wavelength. Note that new intermediate appeared immediately after the $Np(S_1)$ vanished, suggesting that its growth was directly connected with the $Np(S_1) + HNO_2$ reaction. Similarly, by subtracting the Np^+ absorption from the spectrum, the Np–OH absorption again emerged.

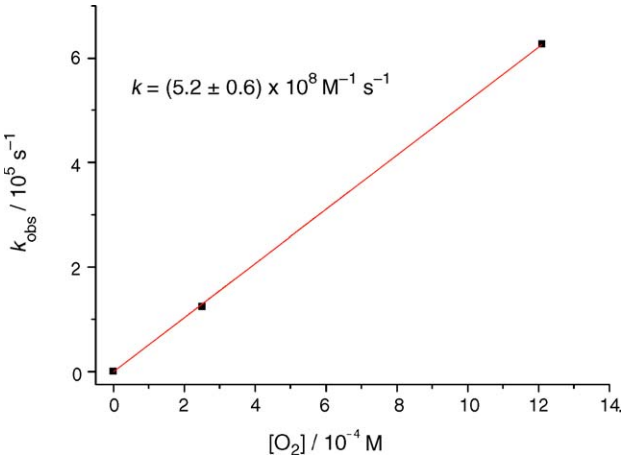

Fig. 10. Linear correlation of the pseudo-first-order decay rate of the intermediate against $[O_2]$.

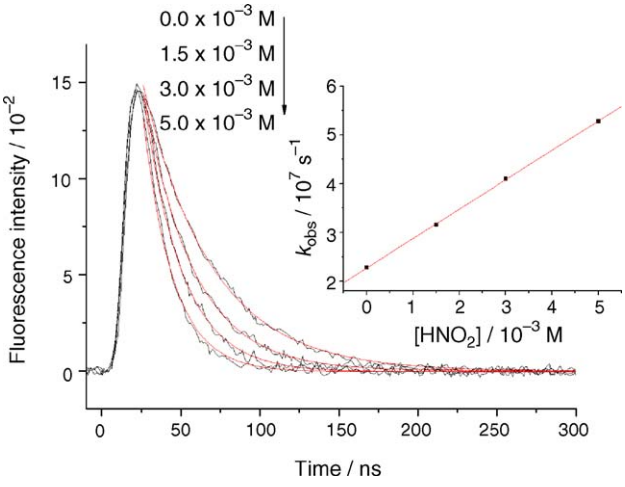

Fig. 11. Acceleration of the decay of the 320 nm fluorescence by adding HNO_2. Inset: linear dependence of the pseudo-first-order decay rate of the fluorescence on $[HNO_2]$.

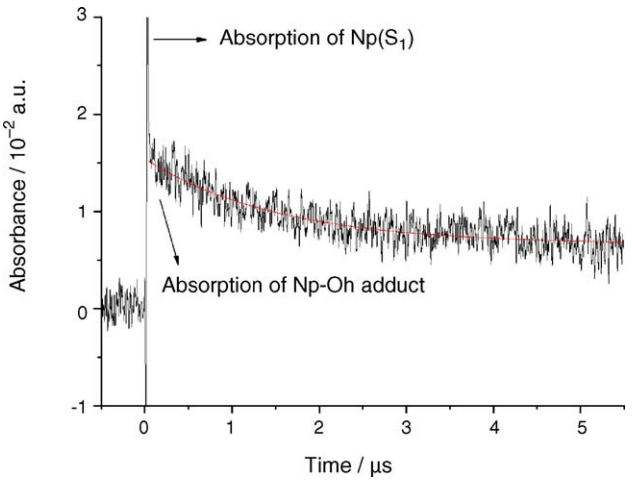

Fig. 12. Transient absorption curve recorded at $\lambda = 290$ nm after the laser flash photolysis of the aqueous solution containing 1.5×10^{-4} M Np and 2×10^{-2} M HNO_2.

It was difficult to directly monitor the synchronous grow and decay processes, because the absorption band of the Np–OH adduct overlapped seriously with the fluorescence region. This cast some uncertainties on the reaction mechanism of $Np(S_1) + HNO_2$, admittedly, as will be discussed in Section 3.4.

3.3.5. *The formation efficiencies (f) of the Np–OH adduct from the Np(T_1) or Np(S_1) + HNO_2 reactions*

Define the formation efficiency of the Np–OH adduct from $Np(T_1)$ and $Np(S_1)$ as f^{T_1} and f^{S_1}, respectively. Here, $f^{T_1} = (c_{Np-OH})/(c_{T_1})$ and $f^{S_1} = (c_{Np-OH})/(c_{S_1})$, where c_{Np-OH} was the amount of Np–OH adduct formed from the quenching of $Np(T_1)$ or $Np(S_1)$ by HNO_2, while c_{T_1} and c_{S_1} were the amount of the $Np(S_1)$ and $Np(T_1)$ consumed.

c_{Np-OH} and c_{T_1} were easy to calculate via (9) and (10).

$$c_{Np-OH} = \frac{A_{Np-OH,320\,nm}}{\varepsilon_{Np-OH,320\,nm} \times l} \quad (9)$$

$$c_{T_1} = \frac{A_{Np(T_1),412\,nm}}{\varepsilon_{Np(T_1),412\,nm} \times l} \quad (10)$$

$A_{Np-OH,320\,nm}$ and $A_{Np(T_1),412\,nm}$ were the peak transient absorbance of the Np–OH adduct at 320 nm and of $Np(T_1)$ at 412 nm, respectively. $\varepsilon_{Np-OH,320\,nm}$ and $\varepsilon_{Np(T_1),412\,nm}$ were the molar extinction coefficients of the Np–OH adduct at 320 nm and of $Np(T_1)$ at 412 nm, i.e. 8200 $M^{-1}\,cm^{-1}$ [11] and 10,050 $M^{-1}\,cm^{-1}$ [20], respectively. l is the analyzing optical path length, 0.65 cm.

c_{S_1} was derived via (11) where Φ_{ISC} was 0.786 [20].

$$c_{Np(S_1)} = \frac{c_{Np(T_1)}}{\Phi_{ISC}} \quad (11)$$

By following the above procedures, f^{T_1} and f^{S_1} were derived to be 0.15 ± 0.01 and 0.11 ± 0.02, respectively.

3.4. *Formation mechanism of the Np–OH adduct in the 266 nm irradiation case*

We first exclude Scheme 2 (266 nm irradiation) from consideration, where the Np–OH adduct was assumed to arise from the 266 nm photolysis of the ground-state complex between Np and HNO_2.

The exclusion was based on the following evidences:

(1) There was no sign of the formation of any ground-state complex between Np and HNO_2, since the UV–vis absorption spectra of the mixed aqueous solution of Np and HNO_2 were exactly the sum of the absorption spectra of Np and HNO_2 recorded individually.
(2) If equilibrium (E.12) does stand, we would expect an increase of the amount of the ground-state complex $[Np\cdots HNO_2]$ when raising the concentration of either Np or HNO_2. This would, according to Scheme 2, ultimately lead to an elevated production of the Np–OH adduct. Nevertheless, as we varied $[HNO_2]$ in the range of 2×10^{-4} M to 2×10^{-2} M, the yield of the Np–OH adduct remained relatively unchanged, again in contradiction with Scheme 2.
(3) According to Scheme 2, the growth rate of the Np–OH adduct should always be equal to k_{14}, no matter the $[HNO_2]$ fluctuated or not. This conflicted with the experimental results, since the growth rate of the Np–OH adduct was found to be strongly dependent on $[HNO_2]$. For details, see Sections 3.3.3–3.3.4 and Fig. 8.

Secondly, we exclude Scheme 3 (266 nm irradiation) from consideration.

The exclusion was based on the following evidences:

(1) The addition of excessive "free" OH scavengers, e.g. ethanol or *iso*-propanol (0.02–0.2 M) exerted no influence on the production of the Np–OH adduct, indicating that virtually no "free" OH radicals were formed. This obviously contradicts with (R.16) in Scheme 3, where the release of "free" OH radical was expected.
(2) HNO_2 was in itself an effective free OH quencher (see (R.3)) and would competitively scavenged OH against Np. Since the total amount of OH was fixed (because the laser

$$Np + HNO_2 \rightleftharpoons [Np\bullet\bullet HNO_2] \quad (E.12)$$

$$[Np\bullet\bullet HNO_2] + h\nu \longrightarrow [Np\bullet\bullet HNO_2]^* \quad (R.13)$$

$$[Np\bullet\bullet HNO_2]^* \xrightarrow{k_{14}} Np\text{-}OH + NO \quad (R.14)$$

Scheme 2.

$$Np^* + HNO_2 \xrightarrow{k_{15}} Np + HNO_2^* \quad (R.15)$$

$$HNO_2^* \longrightarrow OH + NO \quad (R.16)$$

$$OH + Np \xrightarrow{k_2} Np\text{-}OH\ adduct \quad (R.2)$$

Scheme 3.

$$Np^* + HNO_2 \xrightarrow{k_{17}} [Np \bullet\bullet HNO_2]^* \quad (R.17)$$

$$[Np \bullet\bullet HNO_2]^* \xrightarrow{k_{18}} Np\text{-}OH + NO \quad (R.18)$$

$$k_{18} >> k_{17} \times [HNO_2]$$

Scheme 4.

energy was fixed), the increase of $[HNO_2]$ should therefore decrease the production of the Np–OH adduct. This was again negated by experiments, since $[HNO_2]$ up to 2×10^{-2} M (i.e. 100 times as large as [Np]) did not suppress the formation of the Np–OH adduct at all.

(3) The building of the Np–OH adduct, according to Scheme 3, was subjected to three steps. This would clearly lead to very complicated formation kinetics for Np–OH. Nevertheless, we found that the building rate of the Np–OH adduct was constantly exhibiting a simple linear correlation against $[HNO_2]$, and furthermore, was always synchronous with the decay of $Np(T_1)$ or $Np(S_1)$.

We may summarize the two striking characteristics that go with the formation of the Np–OH adduct in the 266 nm irradiation case as follows.

In the first place, no free OH was formed, indicating that the OH group transfer from HNO_2 to Np must have occurred inside a *complex*. Since it was not a ground-state one (as stated vide supra), the complex should bear an excited property.

In the second place, the formation of the Np–OH adduct was always synchronous with the decay of $Np(T_1)$ or $Np(S_1)$ as if the complex were "bypassed". As is well known that for the reaction sequence $A \xrightarrow{k_a} B \xrightarrow{k_b} C$, if the growth rate of final product C coincided well with the decay rate of the starting agent A, we would expect $k_b \gg k_a$. This implied that as soon as the complex was formed, it dissociated very quickly.

To put it more explicitly, we sum up the reaction sequence in Scheme 4 (266 nm irradiation).

The definition of "≫" was to some extent vague. To specify, we define it as "five times larger".

In the $Np(T_1)$ quenching case, the $[HNO_2]_{max}$ applied was 2×10^{-3} M and $k_{17} = 4.8 \times 10^9\ M^{-1}\ s^{-1}$. A lower limit was therefore determined for k_{18}, i.e. $5 \times 10^7\ s^{-1}$ ($5 \times k_{17} \times [HNO_2]_{max}$). This gave an upper limit for the lifetime of the $[Np(T_1) \cdots HNO_2]^*$ exciplex, namely 20 ns.

The $Np(S_1)$ quenching case was more complicated than the $Np(T_1)$ one. It was difficult to directly monitor the growth of the Np–OH adduct on the ground of the serious overlaps of the Np–OH absorptions with both the $Np(S_1)$ absorptions and its fluorescence emissions. But anyway, the Np–OH adduct was formed within 25 ns, as shown in Fig. 12. This value provides an upper limit for the lifetime of the $[Np(S_1) \cdots HNO_2]$ exciplex.

The quick dissociation of the exciplex renders the encounter of Np^* and HNO_2 (R.17) the rate-limiting step in the formation of the Np–OH adduct. Elevation of $[HNO_2]$ would raise $k_{17} \times [HNO_2]$ and may shift the rate-limiting step from the encounter to the dissociation of exciplex. Therefore, the exciplex would accumulate and may possibly be observed by a faster spectroscopy, e.g. the picosecond one.

The formation efficiency of the Np–OH adduct was 0.11 and 0.15 for $Np(S_1)$ and $Np(T_1)$, respectively. Both of the values fall far below unity. Other process, e.g. non-radiative relaxation that leads to the recovery of the parent molecules, must be competing with the dissociation of the exciplex that leads to the production of the Np–OH adduct, as shown in (R.19).

$$\begin{array}{l} Np^* + HNO_2 \longrightarrow [Np \bullet\bullet HNO_2]^* \xrightarrow{\text{dissociation}} Np\text{-OH adduct} \\ \qquad\qquad\qquad\quad \downarrow \text{relaxation} \\ \qquad\qquad\qquad\quad Np + HNO_2 \end{array} \quad (R.19)$$

3.5. Atmospheric implications

Np was ubiquitous in the environment and was among all of the PAHs homologues the most soluble [27] and also the most abundant species in the atmospheric aqueous droplets [28]. Moreover, it may act as a model representative of the PAHs family based on the similarity of molecular and photochemical properties between the homologues.

Photolysis of HNO_2 as a potential OH source in the droplets may contribute to the removal of Np. This conclusion was verified again in this work through the 355 nm irradiation of the mixed aqueous solution of $Np + HNO_2$, where the diffusion-controlled addition of the OH to the Np ring was observed. This, on the other hand, was far from being the only OH-induced removal pathway of Np by HNO_2 in the environment.

As shown in Section 3.3, the excited Np, whatever $Np(T_1)$ or $Np(S_1)$ it may be, is capable of abstracting OH from HNO_2 via forming short-lived exciplex. Since Np absorbs the $\lambda > 290$ nm sunlight (Fig. 1) and thereafter transits to the excited states, this reaction can surely occur in the real tropospheric environment. It was even more important to address that unlike the "free" OH addition pathway in the 355 nm case where the other efficient OH quenchers can effectively suppress the formation of the Np–OH adduct, the exciplex pathway in the 266 nm case was not sensitive to the presence of OH quenchers at all. This liberates Np from the vigorous competition towards OH against the other organic or inorganic free OH scavengers dissolved in the droplets and ensures the latter exciplex pathway be monopolized by Np.

It was not clear yet that whether the aqueous-phase reaction $Np^* + HNO_2$ extends to the gas phase or not. Further works are required to dispel this uncertainty.

4. Conclusions

In this work, we examined the 355 nm and 266 nm laser flash photolysis of the mixed aqueous solution of $Np + HNO_2$. The Np–OH adduct was generated in both cases, but virtually via totally different mechanisms.

Under the 355 nm irradiation, HNO_2 was the only dominant absorber and was photolyzed to release OH with a quantum yield of 0.25. The OH radical thus formed added to the Np ring readily to form the Np–OH adduct.

Under the 266 nm irradiation, Np replaced HNO_2 as the primary absorber and was excited to its S_1 and T_1 state via electronic transition. The Np(S_1) and Np(T_1) both abstracted OH from HNO_2, which resulted again in the formation of the Np–OH adduct. It was further confirmed that the OH abstraction occurred exactly within a short-lived exciplex which, once formed, dissociated very quickly ($>5 \times 10^7\ s^{-1}$).

The above reactions bear potential atmospheric implications because both Np and HNO_2 universally exist in real environment and more importantly, both of them are capable of absorbing the $\lambda > 290$ nm sunlight that available in the troposphere.

Acknowledgements

This work is financially supported by the Research Fund of the Doctorate Program of High Education, PR China (Grant No. 20040246024). We also want to thank Dr. Lei Zhu in the State University of New York at Albany for her constructive comments on the manuscript.

References

[1] R.A. Cox, J. Photochem. 3 (1974) 175.
[2] B.J. Finlayson-Pitts, J.N. Pitts Jr., Atmospheric Chemistry Fundamentals and Experimental Techniques, John Wiley & Sons, New York, 1986.
[3] P. Warneck, Chemistry of the Natural Atmosphere, Academic Press, San Diego, 1988.
[4] M. Fischer, P. Warneck, J. Phys. Chem. 100 (1996) 18749.
[5] T. Arakaki, T. Miyake, T. Hirakawa, H. Sakugawa, Environ. Sci. Technol. 33 (1999) 2561.
[6] D. Vione, V. Maurino, C. Minero, M. Lucchiari, E. Pelizzetti, Chemosphere 56 (2004) 1049.
[7] R. Atkinson, J. Arey, Chem. Rev. 103 (2003) 4605.
[8] C. Vonsonntag, H.P. Schuchmann, Angew. Chem. Int. Ed. Engl. 30 (1991) 1229.
[9] B. Ouyang, W.B. Dong, H.Q. Hou, Chem. Phys. Lett. 402 (2005) 306.
[10] B. Ouyang, R.X. Zhang, C.Z. Zhu, Y.P. Wu, H.Q. Hou, Environ. Chem. 23 (2004) 393 (in Chinese).
[11] N. Zevos, K. Sehested, J. Phys. Chem. 82 (1978) 138.
[12] M. Roder, L. Wojnárovits, G. Földiák, Radiat. Phys. Chem. 36 (1990) 175.
[13] G.V. Buxton, C.L. Greenstock, W.P. Helman, A.B. Ross, J. Phys. Chem. Ref. Data 17 (1988) 513.
[14] T.R. Rettich, Ph.D. Thesis, Case Western Reserve University, 1978.
[15] M.E. Jenkin, R.A. Cox, Chem. Phys. Lett. 137 (1987) 548.
[16] X.Y. Yu, J.R. Barker, J. Phys. Chem. A 107 (2003) 1325.
[17] P.Y. Jiang, Y. Katsumura, R. Nagaishi, M. Domae, K. Ishikawa, K. Ishigure, Y. Yoshida, J. Chem. Soc. Faraday Trans. 88 (1992) 1653.
[18] Y. Katsumura, P.Y. Jiang, R. Nagaishi, T. Oishi, K. Ishigure, Y. Yoshida, J. Phys. Chem. 95 (1991) 4435.
[19] D.O. Cowan, R.L. Drisko, Elements of Organic Photochemistry, Plenum Press, 1976.
[20] G. Grabner, K. Rechthaler, B. Mayer, G. Köhler, K. Rotkiewicz, J. Phys. Chem. 104 (2000) 1365.
[21] D. Bebelaar, Chem. Phys. 3 (1974) 205.
[22] R. McNeil, J.T. Richards, J.K. Thomas, J. Phys. Chem. 74 (1970) 2290.
[23] S. Steenken, C.J. Warren, B.C. Gilbert, J. Chem. Soc. Perkin Trans. II (1990) 335.
[24] D. Vialaton, C. Richard, D. Baglio, A.-B. Paya-Perez, J. Photochem. Photobiol. A 123 (1999) 15.
[25] F. Wilkinson, D.J. McGarvey, A.F. Olea, J. Phys. Chem. 98 (1994) 3762.
[26] C. Schweitzer, Z. Mehrdad, A. Noll, E.W. Grabner, R. Schmidt, J. Phys. Chem. A 107 (2003) 2192.
[27] W.W. Davis, M.E. Krahl, G.H.A. Clowes, J. Am. Chem. Soc. 64 (1942) 108.
[28] J.S. Park, Ph.D. Thesis, Texas A&M University, Texas, 2000.